CHAPTER VI
ENVIRONMENTAL FRIENDLY ROUTE FOR HYDROCARBON AND OXYGENATE PRODUCTION USING Fe- AND Fe_2O_3-PROMOTED γ-ALUMINA CATALYSTS IN CATALYTIC ETHANOL DEHYDRATION

6.1 Abstract

One of the most environmental friendly routes for hydrocarbon production in gasoline range is the catalytic dehydration of bio-ethanol. In this research, metallic Fe-promoted alumina was examined, aiming to examine the formation of oxygenates and hydrocarbons in the catalytic dehydration of bio-ethanol. The amount of Fe loading was fixed at 5 wt%, and prepared by using incipient wetness impregnation technique. The catalyst was characterized using SAA, XRD, XPS, and tested in a continuous fixed-bed U-tube reactor at 500°C under atmospheric pressure. Additionally, the gaseous products were analyzed using GC-online, and the extracted oil were analyzed using GCxGC-TOF/MS in order to identify hydrocarbon species. As a result, it was found that different oxidation states of iron catalysts promoted different dominant reaction. This means that Fe/Al_2O_3 catalyst favoured to promote ethanol dehydration. On the other hand, Fe_2O_3/Al_2O_3 catalyst favoured to promote ethanol dehydrogenation. Moreover, iron catalysts of both metallic and metal oxide promoted similar pathways of ethylene chain growth, and the obtained hydrocarbons were all aromatics. Furthermore, the major components in oxygenate compounds were phenol and 2-pentanone. Additionally, XPS analysis indicated that metallic Fe was entirely transformed to Fe_2O_3 after the catalytic testing.

6.2 Introduction

The depleting in reserve of petroleum oil make the world face with high price of the conventional fuel; that are, gasoline, kerosene, and gas oil. Bio-fuel, especially ethanol, is one of high potential, renewable petroleum substitutes to solve the problems. In the past, hydrocarbons, such as olefins, paraffins, oligomers, and

aromatics, can be produced from fossil fuel, but nowadays the attention has been changed to bio-mass as an alternative source substituted for petroleum, since crude oil price increases continuously. Moreover, there are several disadvantages of crude oil usage such as CO_2 emission, and high energy consumption, which are causes of global warming (Shinohara *et al.*, 1999). In Thailand, there are large quantities of bio-mass such as corn crop, sugar cane, and cassava, which are used to produce bio-ethanol. Furthermore, bio-ethanol can be used as feedstock to produce hydrocarbons such as ethylene, propylene, oligomers, paraffins, and BTEX via catalytic dehydration reaction. Additionally, the other products that can be obtained together with hydrocarbons are oxygenate compounds. Oxygenate compounds can be used in many application such as an additive in petroleum oil. Methyl-Tertiary-Butyl-Ether (MTBE) is used as octane booster to increase octane number, resulting in more complete combustion. Likewise, ethanol is widely used, especially in Thailand, in gasohol product from gasoline, aiming to reduce gasoline prices. On the other hands, oxygenate compounds are not only used as an additive in petroleum oil, but also used as an solvent in many applications. For example, 2-pentanone is used as cleaning agent in medical treatment. Moreover, 3-pentanone is widely used as solvent in painting, and as a precursor for producing vitamin E in drug industry.

Over the decade, Fe catalysts were widely used to produce hydrocarbons in Fischer-Tropsch process. O'Brien *et al.*, (1997) studied the activity and selectivity of precipitated iron catalyst in Fizcher-Tropsch synthesis. They found that iron catalysts gave more than 75% C_2 to C_{11} aliphatic hydrocarbons selectivity. Moreover, Kang *et al.*, (2010) studied Fe catalyst-supported on ZSM-5 in Fischer-Tropsch process, aiming to produce light olefins. The results showed that metallic Fe was an active phase for Fischer-Tropsch process, and it had better selectivity to produce light olefins. Kerosene-range hydrocarbon productions in Fischer-Tropsch synthesis was studied by Kumabe *et al.*, (2010). They found that the reduced Fe preferred to produce olefins than paraffins in C_6+ hydrocarbon range. On the contrary, iron catalysts not only used to produce hydrocarbons but also used to produce oxygenate compounds in various reactions. Guan *et al.*, (2007) studied Fe-supported on SBA-15 catalysts for alcohol dehydration and dehydrogenation. The results showed that iron oxide catalyst favored to promote alcohol dehydrogenation because it had oxygen

vacancies on its surface that allowed the catalysts to abstract hydrogen atom from alcohol molecule. Moreover, they also mentioned that the degree of dehydrogenation depended on the concentration of surface oxygen vacancies. El-katatny *et al.*, (2000) studied FeO_x/Al_2O_3 catalysts for ethanol dehydration from industrial chemical waste. They found that the ethoxy species played an important role to undergo further reactions, and they also revealed that the increasing of FeOx, resulting in the enhancement of oxygenate compounds.

Hence, iron-modified catalysts are an interesting catalyst in the catalytic dehydration of bio-ethanol, since it might have potential to produce oxygenate compounds and hydrocarbons in the catalytic dehydration of bio-ethanol. In this work, iron- and iron oxide-promoted catalysts were examined, aiming to investigate the production of oxygenate compounds and hydrocarbons in the catalytic dehydration of bio-ethanol. Furthermore, the catalysts were characterized using surface area analyzer (SAA), X-ray diffraction spectroscopy (XRD), and X-ray Photoelectron Spectroscopy (XPS).

6.3 Experimental

6.3.1 Catalyst Preparation

γ-Al_2O_3 (γ-Alumina) used in this work was supplied form Sigma Aldrich, Singapore. Iron (III) chloride hexahydrate was used as the iron precursor. A metal solution of iron chloride was loaded on the support using incipient wetness impregnation technique until amount of 5.0 wt% Fe loading was achieved. After impregnation, the wet catalyst was dried at 110°C overnight and then calcined at 600°C, 10°C/min for 3 hours. The calcined catalyst was pelletized, crushed, and sieved to 20-40 mesh particles. For metallic form, the pelletized catalyst was pretreated with H_2 at 650°C for 4 hours.

6.3.2 Catalytic Dehydration of Bio-ethanol

The catalytic dehydration of bio-ethanol was tested in a continuous isothermal fixed-bed U-tube reactor under atmospheric pressure at 500°C with temperature controllers for 8 hours. High purity bio-ethanol (99.5%) was fed by a

syringe pump with carrier gas, helium, thought the catalyst bed. The gaseous products passed through online-GC, and the liquid products received form the reactor were condensed in a cooling unit, and separate the extracted oil was separated by using carbon disulfide.

6.3.3 Product Analysis

The gaseous products were analyzed by using a GC-TCD (Agilent 6890N) to determine the gas composition, and GC-FID (Agilent 6890N) was used to determine the bio-ethanol and oxygenate contents. The extracted oils were analyzed by using Gas Chromatography (Agilent technology 7890) with Time-of-Fight Mass Spectrometer (LECO, Pegasus® 4D TOF/MS) equipped with the 1st GC column was a non-polar Rtx®-5sil MS (30 m × 0.25 mm × 0.25 μm), and the 2nd GC column was an Rxi®-17 MS column (1.790 m × 0.1 mm ID ×0.1 μm) to determine the composition.

6.3.4 Catalyst Characterization

The Brunauer-Emmett-Teller (BET) technique was used to determine the specific surface area, total pore volume, and pore size of catalysts using Thermo Finnigan/Sorptomatic 1990 surface area analyzer. The pore size distribution was calculated using BJH method. The X-ray diffraction of catalysts was determined using RigaguSmartLab® in BB/Dtex mode with CuKα radiation. The machine collected the data from 20°-80° (2θ) at 5°/min with the increment of 0.01°. X-ray Photoelectron Spectroscopy (XPS) spectra were carried out using a AXIS ULTRA^{DLD}. The system was equipped with a monochromatic Al x-ray source and hemispherical analyzer. The spectrometer was operated with the pass energy of 160 and 40 eV for wide and narrow scan, respectively. All peaks were calibrated from referring C 1s spectra located at 284.8 eV.

6.4 Results and Discussion

6.4.1 Characterization of Catalysts

The XRD patterns of catalysts are shown in Figure 6.1. It can be noticed that the peak of γ-alumina can be detected at 2θ =67.5° (Liu *et al.*, 2012). Moreover, the XRD patterns of the calcined and reduced catalysts are shown in Figure 6.1 (B) and (C), respectively. The peaks due to Fe_2O_3 are detected at 2θ = 33.4°, and 35.8° (Park *et al.*, 2010), and the peak due to metallic Fe is detected at 2θ = 44.8° (Wang *et al.*, 2012). Additionally, the peak that represents the characteristics of γ-Al_2O_3 still appear at 2θ = 67.3° in both samples. These mean that Fe_2O_3 is formed on the surface of the alumina catalyst, and metallic Fe is present on the surface of the reduced catalyst. Therefore, the preparation of Fe_2O_3/Al_2O_3 and Fe/Al_2O_3 catalysts was proven successful.

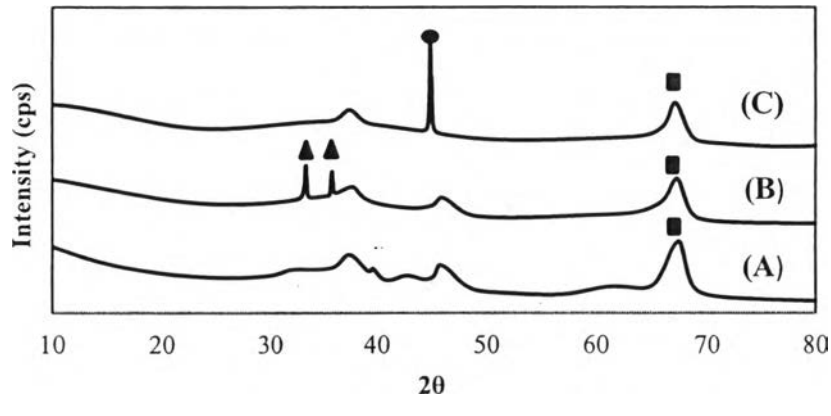

Figure 6.1 XRD pattern of (A) γ-Al_2O_3, (B) Fe_2O_3/Al_2O_3, and (C) Fe/Al_2O_3 (■ = Al_2O_3, ● = Fe, and ▲ = Fe_2O_3).

XPS analysis was employed in order to further verify the chemical species and composition of iron catalysts in both metallic and metal oxide forms, and the results are shown in Figure 6.2 and Table 6.1. The XPS spectrum of fresh Fe/Al_2O_3 catalysts is illustrated in Figure 6.2 (a), the Fe $2p_{3/2}$ peak binding energies of 706.6 and 709.8 eV are assigned to metallic Fe and Fe_2O_3 (Biesinger *et al.*, 2011), accounting for 91.4% and 8.6%, respectively. Moreover, the peaks located at 719.7

and 712.8 eV represent the characteristic satellite of Fe^{2+} and surface peak (Grosvenor *et al.*, 2004). Additionally, the XPS spectrum of spent Fe/Al_2O_3 catalyst is illustrated in Figure 6.2 (b), the Fe $2p_{3/2}$ peak at binding energy of 709.8 eV is assigned to Fe_2O_3 (Biesinger *et al.*, 2011), accounting for 100% Fe_2O_3. The characteristic satellite peak of Fe^{2+} and surface peak are located at 717.7 and 712.9 eV (Grosvenor *et al.*, 2004). Furthermore, it can be concluded metallic Fe/Al_2O_3 catalyst is entirely oxidized to Fe_2O_3 after the catalytic testing. Furthermore, it is well known that metallic Fe is easily oxidized when exposed to the air and oxidizing agent.

In addition, Figure 6.2 (c) displays the XPS spectrum of fresh Fe_2O_3/Al_2O_3 catalyst. The Fe $2p_{3/2}$ binding energy at 709.8 eV is assigned to Fe_2O_3 (Biesinger *et al.*, 2011), accounting for 100% Fe_2O_3. The characteristic of satellite and surface peaks of Fe^{2+} are also observed at 707.2 and 712.9 eV (Grosvenor *et al.*, 2004). Figure 6.2 (d) display the XPS spectrum of spent Fe_2O_3/Al_2O_3 catalyst, it is found that there is no change of binding energy occurs for spent catalyst, and the Fe $2p_{3/2}$ binding energy still locates at 709.8 eV (Biesinger *et al.*, 2011). Moreover, the characteristic of Fe^{2+} and surface peaks are also observed at 716.7 and 712.9 eV (Grosvenor *et al.*, 2004), indicating that Fe_2O_3 is a stable phase of iron oxide. The surface components on both catalysts before and after reaction are shown in Figure 6.3.

Table 6.1 Binding energies (eV) and the surface components of iron- and iron oxide-modified alumina catalysts

Sample		Fe $2p_{3/2}$		Fe $2p_{3/2}$(sat.)		Surface Peak		% Composition	
		Fresh	Spent	Fresh	Spent	Fresh	Spent	Fresh	Spent
Fe/Al_2O_3	Fe	706.6	-	-	-	712.8	712.9	91.4	-
	Fe_2O_3	709.8	709.8	719.7	707.7			8.6	100
Fe_2O_3/Al_2O_3	Fe_2O_3	709.8	709.8	717.2	716.7	712.9	713	100	100

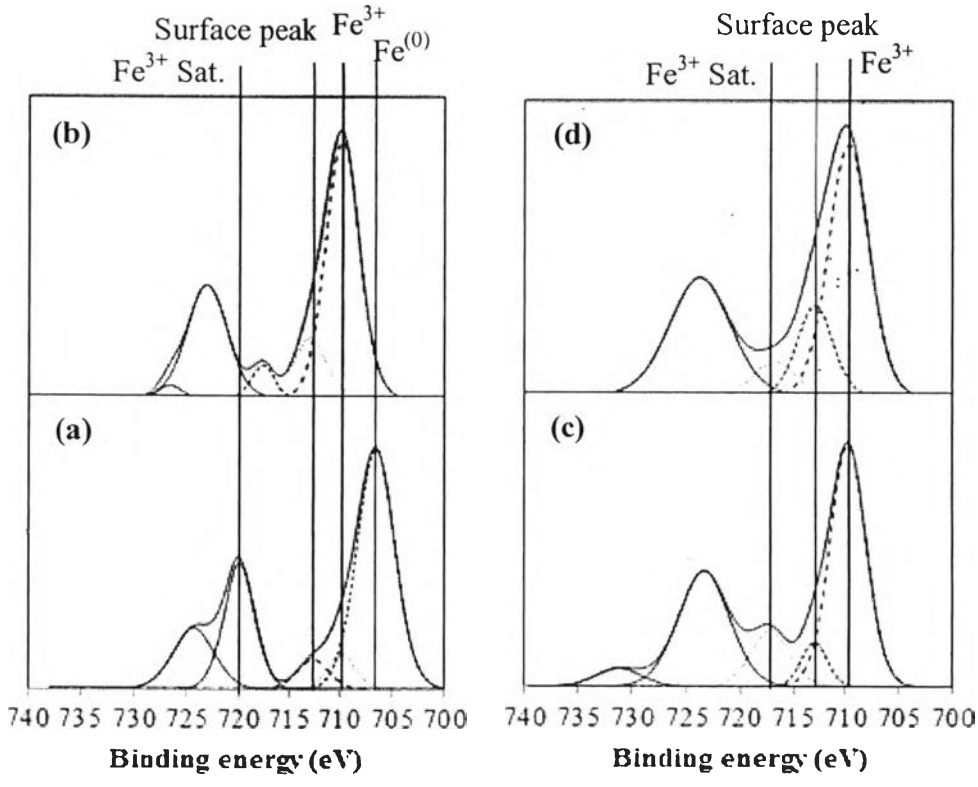

Figure 6.2 XPS spectra of (a) fresh Fe/Al_2O_3, (b) spent Fe/Al_2O_3, (c) fresh Fe_2O_3/Al_2O_3, and (d) spent Fe_2O_3/Al_2O_3.

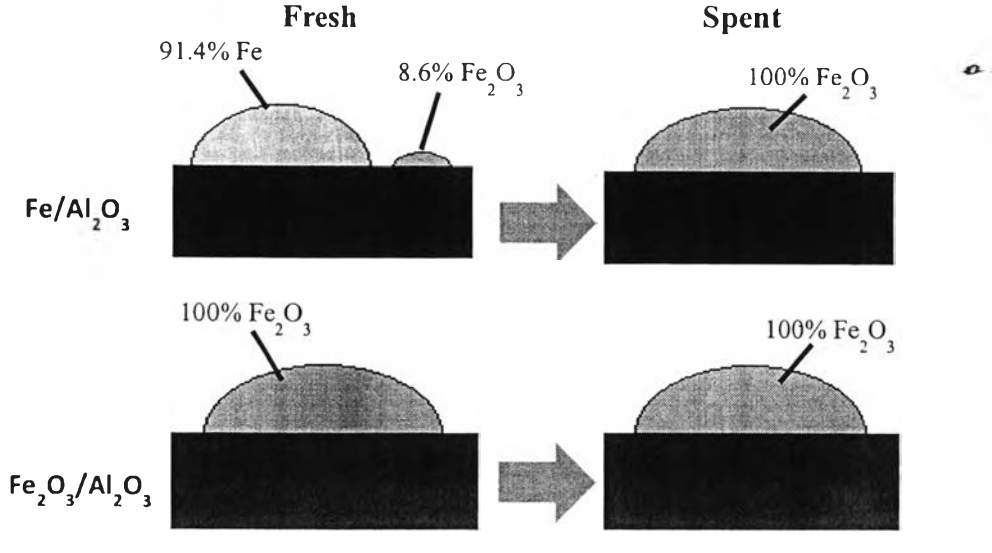

Figure 6.3 Surface compositions of iron- and iron oxide-modified alumina catalysts.

The physical properties of catalyst are present in Table 6.2. Surface area, pore volume, and pore diameter were determined by Barrette-Joyner-Halenda (BJH) and Braunamer-Emmet-Teller (BET) method. As a result, it is found that the formation of metallic Fe and Fe_2O_3 over the alumina surface results in the reduction of surface area. The pore volume and pore diameter do not decrease in the same trend as the surface area.

Table 6.2 Physical properties of Fe-modified catalysts

Catalyst	Surface Area $(m^2/g)^a$	Pore Volume $(cm^3/g)^a$	Pore Diameter $(nm)^b$
Al_2O_3	206.8	0.1792	49.31
Fe/Al_2O_3	190.0	0.1756	26.33
Fe_2O_3/Al_2O_4	147.3	0.1682	45.97

[a] determined using BET method
[b] determined using B.J.H method

6.4.2 Activity of Iron-modified Catalysts

The catalytic dehydration of bio-ethanol using iron-modified catalysts were conducted at 500°C, and bio-ethanol conversion are insignificantly different form all catalysts. Table 6.3 displays the product yield of oil, water, and gas obtained from using Fe/Al_2O_3, and Fe_2O_3/Al_2O_3 catalysts. It is found that the yield of oil and water are slightly decreased; however, the gas yield is slightly increased as compared to unmodified Al_2O_3, indicating that Fe-modified catalysts favor to produce gaseous products.

Table 6.3 Product yields obtained from using Fe-modified catalysts.

Sample	% Yield			Conversion
	Oil	Water	Gas	
Non-catalyst	6.2	11.2	82.6	99.2
Al_2O_3	3.1	20.6	76.3	98.7
Fe/Al_2O_3	2.7	8.4	88.9	97.4
Fe_2O_3/Al_2O_3	3.4	17.6	89.0	98.3

The gaseous product compositions obtained by using Al_2O_3 with Fe and Fe_2O_3 promoters seem to be the same composition as obtained from un-promoted Al_2O_3. As a result, it is found that ethylene is made dominantly from all catalysts. Compared to pure Al_2O_3, ethylene is slightly suppressed from 96.0 wt% to 78.6 wt% and 82.7 wt% by using Fe/Al_2O_3 and Fe_2O_3/Al_2O_3, respectively. Moreover, the other gaseous co-products, for examples, are methane, ethane, propylene, and butylene present in a trace amount. This can be assumed that ethylene that decreases in the gaseous product might convert to be hydrocarbons in oily product.

The yield of oxygenate compounds and hydrocarbons are analyzed using GC×GC-TOF/MS, and the results are displayed in Figure 6.3. It is found that the extracted oil is composed of oxygenate compounds and hydrocarbons. With using different oxidation states of iron promoters, catalysts are selective to produce different products. Compared to parent Al_2O_3, the hydrocarbons are significantly increased from 7.9 wt% to 22.3 wt% using Fe/Al_2O_3, and the oxygenate compounds are slightly increased form 92.1 wt% to 95.0 wt% using Fe_2O_3/Al_2O_3. This indicated that oxidation state has the effect on the product distributions. Moreover, the oxygenate selectivity can be ranked in the order of Al_2O_3 > Fe_2O_3/Al_2O_3>Fe/Al_2O_3; however, the hydrocarbon selectivity can be ranked in reverse order.

Table 6.4 Oxygenates and hydrocarbons found from using Fe catalysts

Catalyst	Product Distribution (wt%)	
	Oxygenates	Hydrocarbons
Non-catalyst	89.0	11.0
Al_2O_3	92.1	7.9
Fe/Al_2O_3	77.7	22.3
Fe_2O_3/Al_2O_3	95.0	5.0

Table 6.5 Gaseous products distribution from using Fe-modified catalysts

Catalyst	Concentration (wt%)							
	CH_4	C_2H_4	C_2H_6	C_3H_6	C_3H_8	C_4H_8	C_4H_{10}	CO_2
Non-catalyst	0.0	99.1	0.6	0.2	0.0	0.1	0.0	0.0
Al_2O_3	0.0	96.0	0.5	1.0	0.0	0.5	0.0	2.1
Fe/Al_2O_3	3.1	78.6	2.4	2.4	0	0.8	0.0	12.1
Fe_2O_3/Al_2O_3	2.3	82.7	1.9	1.7	0	0.6	0.0	10.8

Data were taken at the eight hour of time-on-stream

Table 6.6 Compositions of hydrocarbons (wt%) obtained from using Fe-modified catalysts

Product	Sample			
	Non-catalyst	A_2O_3	Fe/Al_2O_3	Fe_2O_3/Al_2O_3
Product Distribution (wt%)				
Oxygenates	89.0	92.1	77.7	95.5
Non-aromatics	1.44	0.60	0.00	0.00
Benzene	4.28	5.20	17.3	2.60
Toluene	0.31	0.60	1.10	0.10
p-Xylene	0.20	0.20	0.30	0.10
o-Xylene	0.02	0.20	0.20	0.10
m-Xylene	0.03	0.20	0.30	0.10
Ethylbenzene	0.12	0.40	0.50	0.40
C_9 aromatics	0.10	0.10	1.40	0.70
C_{10}^+ aromatics	4.53	0.40	1.10	0.60

Data were taken at the eight hour of time-on-stream

The liquid product composition in Table 6.4 shows that all Fe-modified catalysts give nearly the same hydrocarbon compositions as those obtained from unmodified Al_2O_3. In addition, the hydrocarbons are composed of benzene, toluene, mixed-xylenes, C_9, and C_{10}^+-aromatics. Moreover, it can be observed that there is no non-aromatic formation by using both Fe/Al_2O_3 and Fe_2O_3/Al_2O_3 catalysts. This can be explained that ethylene suppressed in the gaseous product is suspected to be an important intermediate to transform to hydrocarbons in oil via

ethylene aromatization, resulting in the formation of benzene as a primary hydrocarbon in oil. From Figure 6.3, it can be observed that most of the hydrocarbons are distributed in C_6 products; that is benzene, and the maximum carbon number is C_{13}.

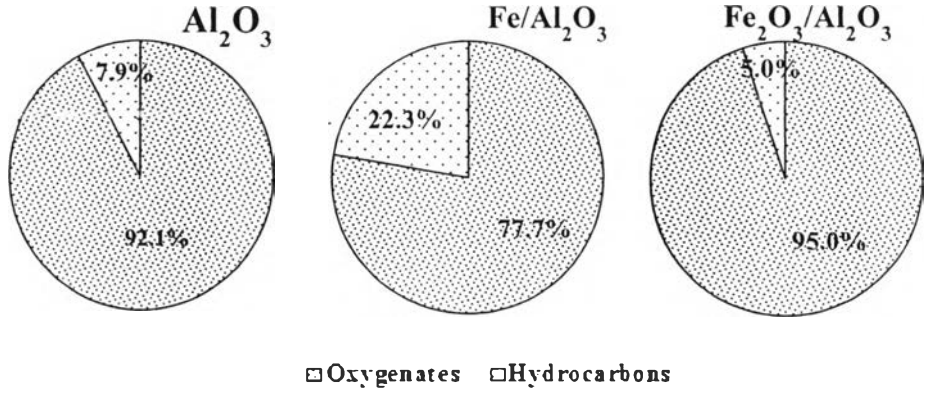

(a)

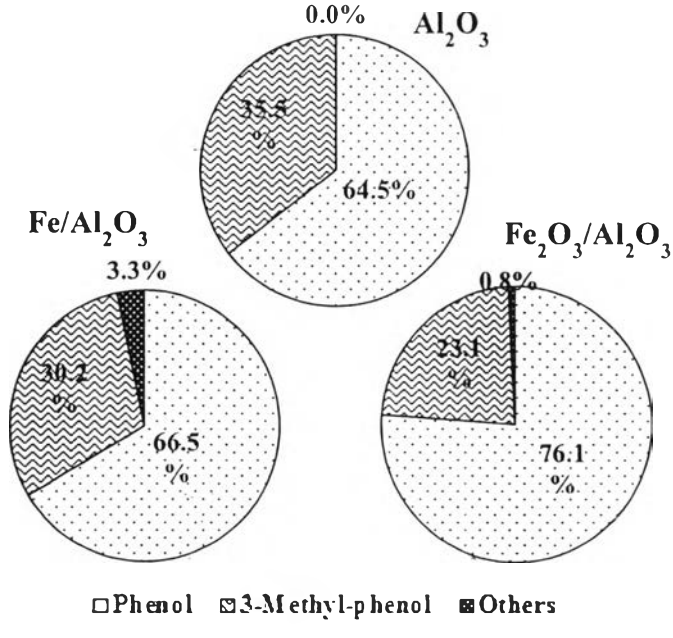

(b)

Figure 6.4 (a) Liquid product distribution, and (b) Compositions of oxygenate compounds (wt%) using Fe-modified catalysts.

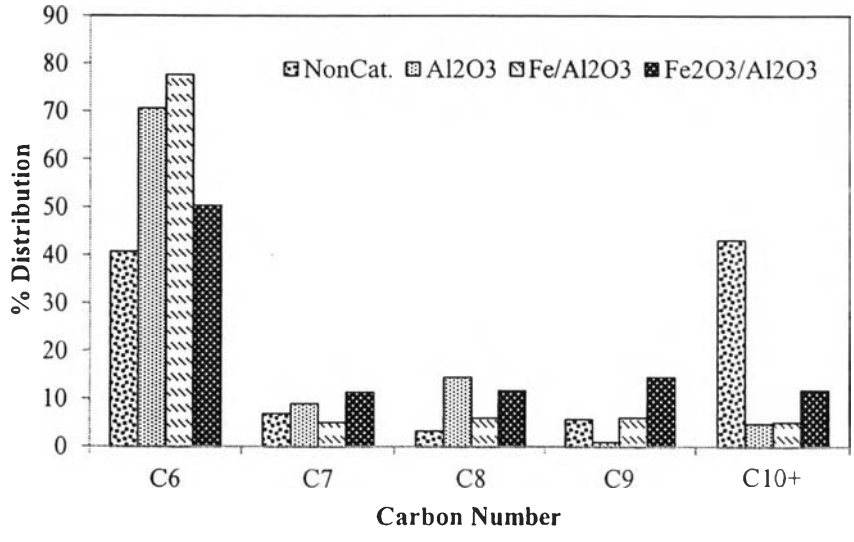

Figure 6.5 Carbon number distribution in oils from using Fe-modified catalysts.

Table 6.7 Compositions in oxygenate compounds from using Fe-modified catalysts

Sample	Product Distribution (wt%)		
	Phenols	Ketones	Others
Al_2O_3	64.5	35.5	0.0
Fe/Al_2O_3	74.4	24.9	0.7
Fe_2O_3/Al_2O_3	76.1	23.1	0.7

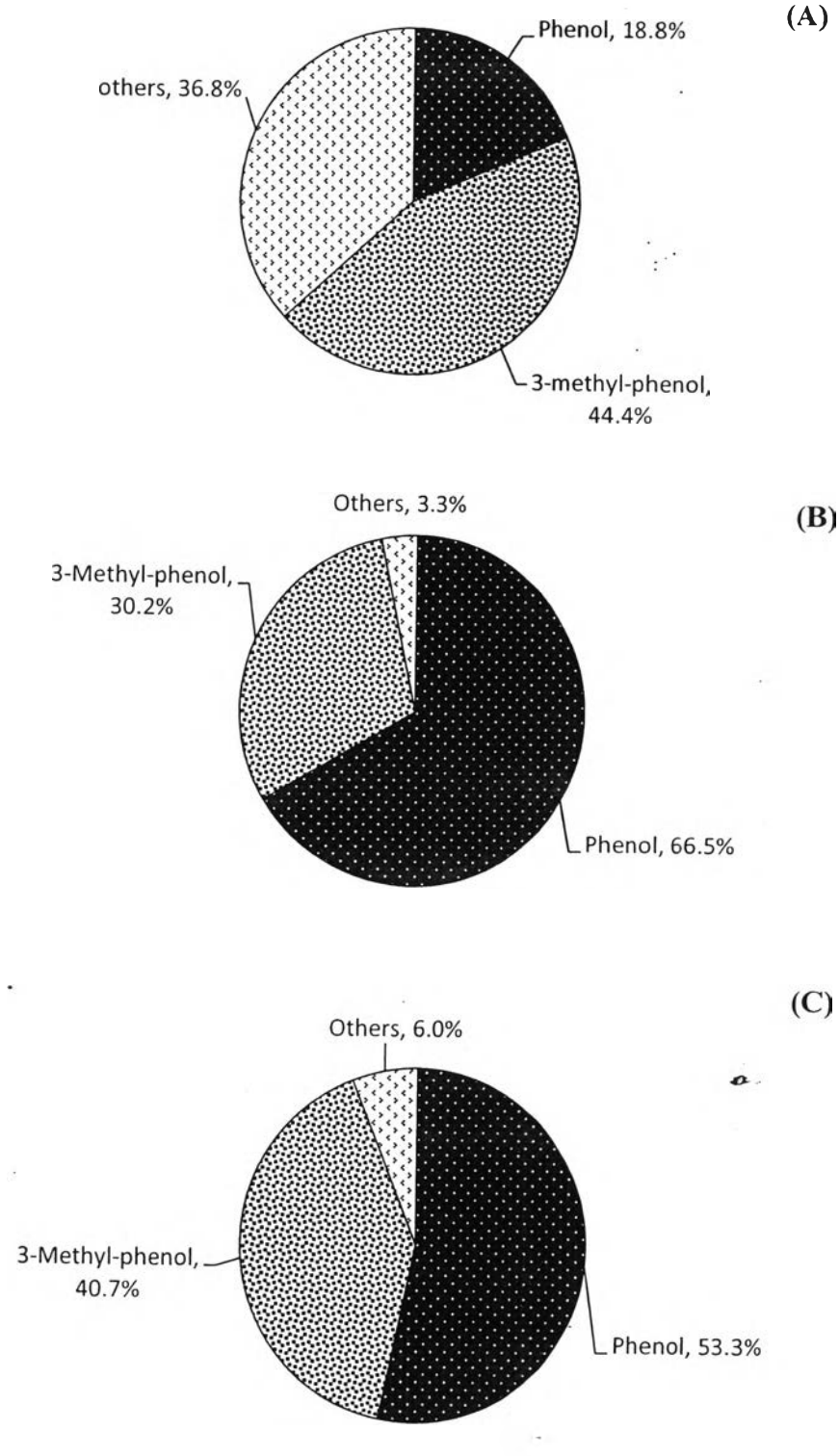

Figure 6.6 Compositions of phenols (wt%) in oxygenate compounds: (A) Al_2O_3, (B) Fe/Al_2O_3, and (C) Fe_2O_3/Al_2O_3.

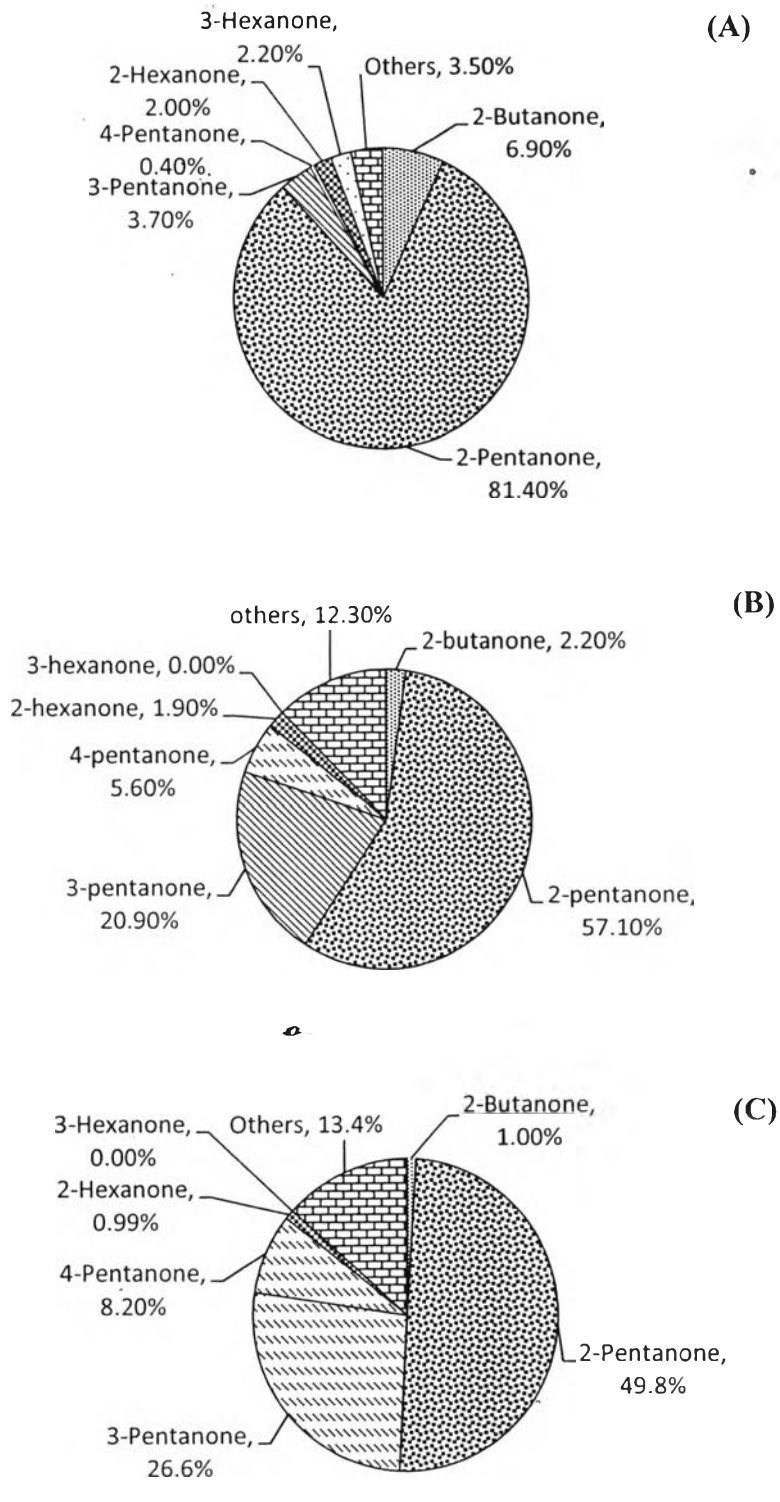

Figure 6.7 Compositions of ketones (wt%) in oxygenate compounds: (A) Al_2O_3, (B) Fe/Al_2O_3, and (C) Fe_2O_3/Al_2O_3.

6.4.3 Oxygenate Compounds Production

The composition of oxygenate compounds obtained from the catalytic dehydration of bio-ethanol are displayed in Table 6.7. It is found that oxygenate compounds obtained by using Fe-modified catalyst are composed of mainly phenol and ketone compounds. Moreover, the others are a trace amount of ethers. As a result, phenol products are increased to 74.4 wt% and 76.1 wt% by using Fe/Al_2O_3, and Fe_2O_3/Al_2O_3, respectively. However, ketone compounds are decreased from 35.5 wt% to 24.9 wt% and 23.1 wt% using Fe/Al_2O_3 and Fe_2O_3/Al_2O_3 catalysts. Compared to Al_2O_3, phenol selectivity can be ranked as follows: Fe_2O_3/Al_2O_3 > Fe/Al_2O_3 > Al_2O_3, and ketone selectivity can be ranked as follows: Al_2O_3 > Fe/Al_2O_3 > Fe_2O_3/Al_2O_3.

Figure 6.6 shows that the majority of oxygenate compounds is phenol products, which holds over 50% of total oxygenate compounds obtained from all modified catalysts. In phenol compounds, phenol that has high cost and can be used in many applications is found as the main component. Among all catalysts, Fe/Al_2O_3 catalyst gave the highest phenol selectivity, followed by with Fe_2O_3/Al_2O_3 catalyst, and then parent Al_2O_3. Therefore, phenol selectivity can be ranked as follows: Fe/Al_2O_3>Fe_2O_3/Al_2O_3>Al_2O_3.

Furthermore, ketone compounds are found as the major co-component in oxygenate compounds. The compositions of ketone compounds obtained from using Fe/Al_2O_3 and Fe_2O_3/Al_2O_3 are as same as obtained from parent Al_2O_3 as shown in Figure 6.7. Additionally, 2-pentanone is found as a major component from all catalysts. Using Fe/Al_2O_3 and Fe_2O_3/Al_2O_3, 2-pentanone is decreased from 81.4 wt% to 57.1 wt% and 49.8 wt%; however, 3-pentanone is significantly increased from 3.7 wt% to 26.0 wt% and 26.6 wt%, respectively. From the results, 2-pentanone selectivity can be ranked in the order of Al_2O_3 > Fe/Al_2O_3 > Fe_2O_3/Al_2O_3, and 3-pentanone can be ranked in the order of Fe/Al_2O_3 = Fe_2O_3/Al_2O_3 > Al_2O_3.

From the result, it can be noticed that all catalysts give nearly the same oxygenate compounds composition; that are, composed of phenol, ketone, and trace amount of ether products, in the near neighborhood (Figure 6.4b). This indicates that all catalysts might promote similar pathways of oxygenate compounds

formation, and the possible mechanisms are illustrated in Figure 6.8 and 6.9, respectively.

6.4.4 Effect of Oxidation State of Iron

The catalytic dehydration of bio-ethanol using different oxidation states of iron promoter on alumina catalysts was examined, aiming to investigate the effect of oxidation state on product distribution. From our study, it is revealed that different oxidation states of iron promoters could promote different pathways of ethanol transformation, and affected to product distribution. The possible reaction pathways can be drawn as illustrated in Figure 6.10. As a result, using Fe/Al_2O_3, hydrocarbon formations were significantly enhanced as compared to unmodified Al_2O_3; so, the possible reaction is driven to Pathway (B), meaning that ethanol is undergone dehydration reaction to form ethylene, and converted to other hydrocarbons in oil. Although hydrocarbons are significantly increased, but oxygenate compounds are still the main component in oil. This can be explained that γ-Al_2O_3 is classified as one kind of metal oxide, which contains oxygen vacancy on its surface; so, they can promote ethanol dehydrogenation pathway along with dehydration of ethanol. Additionally, the use of Fe_2O_3/Al_2O_3catalyst exhibits the opposite pathways of ethanol transformation because the oxygenate compounds are slightly enhanced. This can be explained that most of ethanol might undergo dehydrogenation over the metal oxide catalyst, resulting in the formation of aldehyde as primary oxygenate compounds. Moreover, aldehyde can undergo further reactions, which lead to the formation of phenol and ketone compounds having aldor species as important intermediate.

From the results, it can be concluded that different oxidation states selectively produce different products, and promote different reactions. As a result, loading metallic Fe on Al_2O_3 enhances the dehydration of ethanol, resulting in the increasing formation of hydrocarbons; however, loading Fe_2O_3 on Al_2O_3 instead promotes dehydrogenation of ethanol, resulting in the increasing formation of oxygenate compounds.

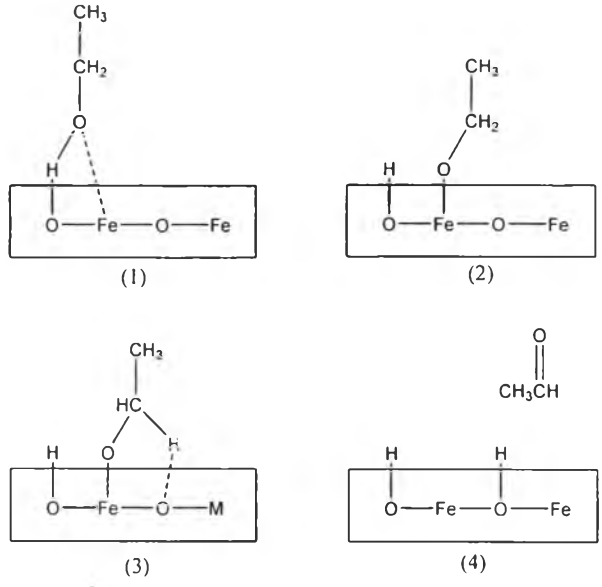

Figure 6.8 Mechanism of acetaldehyde formation.

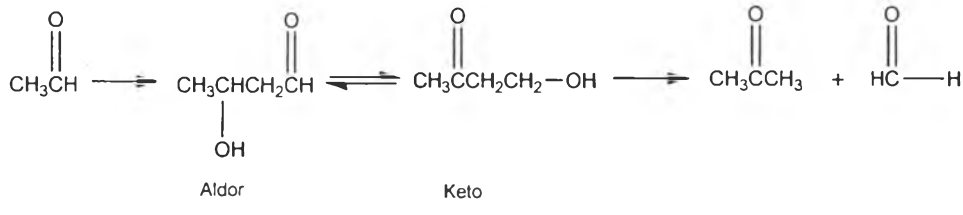

Figure 6.9 Transformation of aldor species to acetone (He *et al.*, 2005).

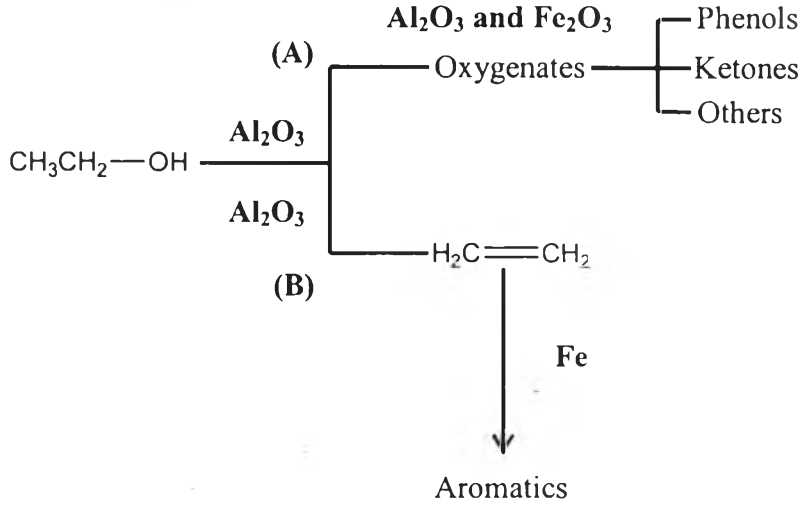

Figure 6.10 Ethanol transformation pathways from using Fe-modified catalysts.

6.5 Conclusions

In summary, it was found that different oxidation states of iron catalysts promoted different reaction pathways, and selectively produce different products. As compared to parent alumina, metallic Fe/Al_2O_3 catalyst selectively produced hydrocarbons rather than oxygenated compounds, and promoted ethanol dehydration as the dominant reaction pathways. Hydrocarbons were distributed in C_6 products, and they were totally aromatics without non-aromatic formation. Moreover, benzene was found as the dominant hydrocarbon product in oil. On the other hand, Fe_2O_3/Al_2O_3 catalyst selectively produced oxygenated compounds rather than hydrocarbons, and promoted ethanol dehydrogenation as the dominant reaction pathway. Additionally, the oxygenate compounds were composed of phenols and ketones. Furthermore, both metallic iron and iron oxide catalysts promoted the similar pathways of ethylene chain growth via ethylene aromatization reaction

6.6 References

Biesinger, M.C., Payne, B.P., Grosvenor, A.P., Lau, L.W.M., Gerson, A.R., and Smart, R.S.C. (2011) Resolving surface chemical states in XPS analysis of first row transition metals, oxides and hydroxides: Cr, Mn, Fe, Co and Ni. Applied Surface Science, 257(7), 2717-2730.

El-Katatny, E.A., Halawy, S.A., Mohamed, M.A., and Zaki, M.I. (2000) Recovery of ethene-selective FeO_x/Al_2O_3 ethanol dehydration catalyst from industrial chemical wastes. Applied Catalysis A: General, 199(1), 83-92.

Grosvenor, A.P., Kobe, B.A., Biesinger, M.C., and McIntyre, N.S. (2004). Investigation of multiplet splitting of Fe 2p XPS spectra and bonding in iron compounds. Surface and Interface Analysis, 36(12), 1564-1574.

Guan, Y., Li, Y., van Santen, R., Hensen, E.M., and Li, C. (2007) Controlling Reaction Pathways for Alcohol Dehydration and Dehydrogenation over FeSBA-15 Catalysts. Catalysis Letters, 117(1-2), 18-24.

He, D., Ding, Y., Chen, W., Lu, Y., and Luo, H. (2005) One-step synthesis of 2-pentanone from ethanol over K-Pd/MnOx-ZrO_2-ZnO catalyst. Journal of Molecular Catalysis A: Chemical, 226(1), 89-92.

Kang, S.-H., Ryu, J.-H., Kim, J.-H., Sai Prasad, P.S., Bae, J., Cheon, J.-Y. and Jun, K.-W. (2011) ZSM-5 Supported Cobalt Catalyst for the Direct Production of Gasoline Range Hydrocarbons by Fischer–Tropsch Synthesis. Catalysis Letters 141, (10), 1464-1471.

Kumabe, K., Sato, T., Matsumoto, K., Ishida, Y. and Hasegawa, T. (2010) Production of hydrocarbons in Fischer–Tropsch synthesis with Fe-based catalyst: Investigations of primary kerosene yield and carbon mass balance. Fuel 89 (8), 2088-2095.

Liu, C., Li, J., Zhang, Y., Chen, S., Zhu, J., and Liew, K. (2012) Fischer–Tropsch synthesis over cobalt catalysts supported on nanostructured alumina with various morphologies. Journal of Molecular Catalysis A: Chemical, 363–364, 335-342.

O'Brien, R.J., Xu, L., Spicer, R.L., Bao, S., Milburn, D.R. and Davis, B.H. (1997) Activity and selectivity of precipitated iron Fischer-Tropsch catalysts. Catalysis Today 36(3), 325-334.

Park, J.-Y., Lee, Y.-J., Khanna, P.K., Jun, K.-W., Bae, J.W., and Kim, Y.H. (2010) Alumina-supported iron oxide nanoparticles as Fischer–Tropsch catalysts: Effect of particle size of iron oxide. Journal of Molecular Catalysis A: Chemical, 323(1–2), 84-90.

Shinohara, Y., Nakajima, T., and Suzuki, S. (1999) A theoretical study of the dehydration and the dehydrogenation processes of alcohols on metal oxides using MOPAC. Journal of Molecular Structure: THEOCHEM, 460(1–3), 231-244.

Wang, L., Hisada, Y., Koike, M., Li, D., Watanabe, H., Nakagawa, Y., and Tomishige, K. (2012) Catalyst property of Co–Fe alloy particles in the steam reforming of biomass tar and toluene. Applied Catalysis B: Environmental, 121–122, 95-104.